ACS OMEGA

http://pubs.acs.org/journal/acsodf

Article

Investigation of Pyrolysis and Mild Oxidation Characteristics of Tar-Rich Coal via Thermogravimetric Experiments

Li Ma, Qisen Mao, Chang'an Wang,* Zhonghui Duan, Meijing Chen, Fu Yang, Jiamiao Liu, Zhendong Wang, and Defu Che

Cite This: *ACS Omega* 2022, 7, 25613−25624

Read Online

ACCESS | Metrics & More | Article Recommendations

ABSTRACT: Tar-rich coal has the potential to substitute the supply of oil-gas resources, which is abundant in China. The effective conversion of tar-rich coal into oil-gas products can promote coal utilization, reduce resource wastage, alleviate environmental pollution, and benefit carbon neutrality. Nevertheless, less work, if any, has been performed on the pyrolysis and mild oxidation behaviors of tar-rich coal in Northwestern China. The influences of limited oxygen addition and an extremely low heating rate on the micromorphology of the residual semi-coke are yet to be fully understood. Here, an experimental study on the pyrolysis and mild oxidation characteristics of tar-rich coal was conducted by the thermogravimetric analysis method, with further elucidation of the physical−chemical properties of the residual semi-coke. Experimental results show that an increase in the ultimate temperature of pyrolysis leads to a decline in the residue mass, while the mass loss from 500 to 550 °C presents the maximum elevation. Volatile matter is inclined to discharge from a certain direction, and the pores formed in various directions hold different possibilities. The organic components undergo both pyrolysis and slow oxidation with limited oxygen in the heating medium. Compared with an inert atmosphere, the mass loss under conditions of a small amount of O_2 is brought forward but prolonged. Compared with a N_2 atmosphere, the oxidation reactions of tar-rich coal are weakened in the presence of CO_2. A large decrease in the heating rate exerts an unfavorable effect on the production of total volatiles. An extremely low heating rate possibly brings about a change in the mechanism of chemical bond cracking during pyrolysis. More pores can be yielded in tar-rich coal with an increase in the heating rate, and the morphology of the residual semi-coke after pyrolysis is susceptible to the heating rate. The present study offers an improved understanding of the pyrolysis characteristics of tar-rich coal as well as insights into the efficient utilization of tar-rich coal.

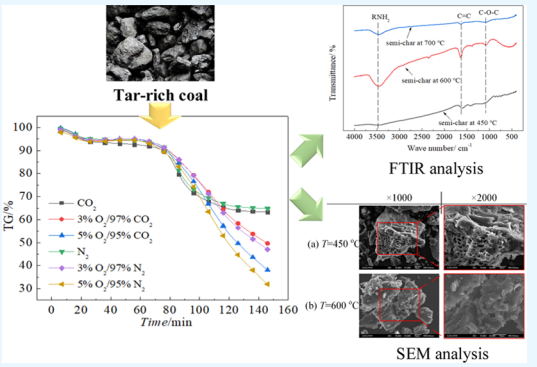

1. INTRODUCTION

Coal makes an important contribution to the global energy consumption,[1,2] whereas the energy structure of China has a feature of "rich in coal, short in oil, and little gas". Hence, coal has always played a predominant role in the chemical industry and in electricity generation.[3,4] In China, the external dependencies for crude oil and natural gas were 73.5 and 43.2% in 2020,[5] respectively, which generate a potential threat to the security of energy supply and socioeconomic development. Moreover, future coal utilization should demonstrate substantially reduced environmental influences.[6] Coal is a valuable source to derive oil−gas products and high-value-added chemicals, whereas tar-rich coal holds a clear advantage in substituting the supply of oil and gas resources. Tar-rich coal is described as coal with a tar yield of 7−12% (7% < Tar_d < 12%). According to the tar yield at temperatures from 500 to 700 °C, coal can be roughly classified into tar-containing coal ($Tar_d \leq 7\%$), tar-rich coal (7% < Tar_d < 12%), and high-tar coal ($Tar_d \geq 12\%$), respectively,[5,7,8] which is an extensively used definition method in coal geology.

Tar-rich coal is not only a type of coal but also a kind of coal-based oil−gas resource.[5] Northwestern China is extremely abundant in tar-rich coal. The five provinces in Northwestern China, including Shaanxi, Xinjiang, Ningxia, Gansu, and Inner Mongolia, have over 500 billion tons of tar-rich coal.[9,10] If the tar-rich coal is appropriately exploited and utilized, plentiful oil−gas resources can be derived, which is extremely consequential for China in the absence of enough conventional oil−gas resources. It is essential to change the coal attribute of tar-rich coal into a coal-based oil−gas attribute rather than

Received: May 5, 2022
Accepted: June 29, 2022
Published: July 13, 2022

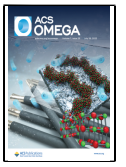

direct combustion of tar-rich coal. Hence, the efficient and clean technology of oil−gas production from tar-rich coal should be further developed, which can contribute to the goal of carbon peaking and carbon neutrality. The conversion of tar-rich coal into oil−gas products can enhance the coal utilization rate, decline resource wastage, and promote environmental safety.[11,12]

Oil can be produced from traditional coal pyrolysis and coal-to-liquid (CTL) technologies above the ground, such as coal carbonization, direct coal liquefaction, and indirect coal liquefaction, which have been extensively investigated in the past few decades.[13−15] These well-known aboveground technologies also bring about possible environmental pollution and excessive semi-coke production,[8,16,17] such as particle matter emission, gaseous emission, and coking wastewater, which do not fulfill the requirements of energy security and carbon neutrality nowadays. Consequently, the underground in situ pyrolysis technology of tar-rich coal has been proposed recently. Without exploitation, the tar-rich coal is heated and pyrolyzed underground through a heat carrier medium, and then the oil−gas products are transported to the ground followed by the subsequent separation and further processing. Unlike the aboveground technologies, only oil and gas are extracted from the tar-rich coal directly, with solid semi-coke left underground for future exploitation or CO_2 sequestration. The in situ pyrolysis technology of tar-rich coal has the advantages of environmental friendliness, sustainability, carbon reduction, capacity increase for potential CO_2 sequestration within residual semi-coke, etc.[6] Nevertheless, challenges are still encountered due to the extremely different conditions between aboveground and underground circumstances, such as the high pressure, nonuniformity of the coal seam, broad scale, difficulty of effective heat transfer, and precise temperature control underground. Indeed, the new in situ pyrolysis technology emphasizes the use of coal-based oil−gas production rather than traditional coal mining. The char matrix left underground is a potential reservoir for CO_2 sequestration due to the considerable increase in the surface area of semi-coke after the in situ pyrolysis, which is likely to induce "carbon neutrality".[18] In addition, investigators at the University of Utah also performed a few studies on the underground in situ coal thermal treatment for synthetic fuel production;[6,18,19] however, they mainly focused on deeply buried coal seams that are uneconomical through the traditional mining approach, instead of tar-rich coal.

Many efforts have been devoted to coal pyrolysis in the past few decades. Okumura[20] investigated the influences of the coal type and heating rate on the yields of functional coal-tar components and indicated that the tar yield had a positive linear correlation with the H/C atomic ratio within the coal. Song et al.[21] probed the pyrolysis characteristics and kinetics of low-rank coals through thermogravimetric analysis at heating rates of 5, 10, 20, and 30 °C·min^{-1} to estimate pyrolysis processes of coal samples. They also captured various carbon functional groups in macromolecular structures of low-rank coals. However, they did not place emphasis on pyrolysis at an extremely low heating rate. Gneshin et al.[6] examined structural changes in the porous network of very large particles of Utah bituminous coal undergoing pyrolysis under atmospheric pressure and at a heating rate as low as 0.1 °C·min^{-1}, and they observed an absence of plastic deformation at heating rates below 10 °C·min^{-1}. Kelly et al.[19] evaluated the life-cycle energy and greenhouse gas (GHG) impacts of underground coal thermal treatment (UCTT) in all processing stages, and they found that GHG emission of UCTT technology was in the range of in situ pyrolysis of oil shale. Wang et al.[22] developed a modified CPD model to predict coal devolatilization under conditions of underground coal thermal treatment (UCTT) at a low temperature and low heating rate.

The heating rate exerts a considerable influence on mass loss behaviors during the pyrolysis process. Huanying et al.[23] emphasized the effects of CO_2 and H_2O on coal pyrolysis at the ultrafast heating rate of around 1800 °C·min^{-1} in a concentrating photothermal reactor, rather than by the traditional thermogravimetry analysis (TGA). They demonstrated that coal pyrolysis was promoted by CO_2 within 50% concentration and the addition of H_2O into 30% CO_2 at an ultrafast heating rate. Xu et al.[24] indicated that the tar from coal pyrolysis became heavier at a higher heating rate, whereas coal pyrolysis produced more light tar at higher pyrolysis temperatures. Duan et al.[25] also reported that an increased heating rate was beneficial for coal pyrolysis reactions, whereas an elevated pyrolysis rate of coal could significantly increase the yield of light gases.[26] Yan et al.[27] believed that the yield of light gases could be enhanced by increasing the ultimate temperature and the heating rate. Wu et al.[28] indicated that variations in the heating rate mainly affected the primary pyrolysis stage (450−550 °C) of perhydrous coals, whereas Strezov et al.[29] found that the endothermic reaction related to secondary devolatilization was the strongest at temperatures ranging from 500 to 600 °C. Ju et al.[8,30] proposed the utilization of an intelligent unmanned automatic mining machine with microwave pyrolysis technology for the in situ conversion of coal resources into oil−gas products.

Although extensive studies have been performed on the pyrolysis of oil shale and coal, few efforts, if any, have been devoted to the study of pyrolysis and mild oxidation of tar-rich coal in Northwestern China. Several fluid mediums, including N_2, CO_2, flue gas, water vapor, etc., can be utilized to heat tar-rich coal underground, while the different effects of the various heating media are still unclear. The addition of a small amount of oxygen into inert heating mediums possibly has a substantial influence on the pyrolysis process, which also requires to be further elucidated. Moreover, the heating rate of the underground in situ pyrolysis is possibly quite low, but previous work mainly emphasized the effects of high and medium heating rates. Here, the pyrolysis and mild oxidation characteristics of tar-rich coal were experimentally explored, including a low pyrolysis temperature, varied pyrolysis atmospheres, and an extremely low heating rate. The impacts of limited oxygen addition into the pyrolysis fluid medium were also elucidated. The physical−chemical properties of residual semi-coke have significant influences on the potential for CO_2 sequestration and subsequent utilization. Hence, the influences of varied pyrolysis conditions on residual semi-coke from tar-rich coal were further clarified. The present study can offer useful information on pyrolysis and mild oxidation characteristics of tar-rich coal, which helps promote the efficient utilization of tar-rich coal to produce oil−gas resources and benefits carbon neutrality.

2. EXPERIMENTAL SECTION

2.1. Sample. In the present study, a typical tar-rich coal from the Northern Shaanxi region was chosen to conduct the investigation. The experimental sample was sieved to a particle size of less than 125 μm. The chemical properties of solid

https://doi.org/10.1021/acsomega.2c02786
ACS Omega 2022, 7, 25613−25624

Table 1. Proximate and Ultimate Analyses of the Experimental Sample

proximate analysis/%				ultimate analysis/%				
FC_{ad}	M_{ad}	A_{ad}	V_{ad}	C_{daf}	H_{daf}	N_{daf}	O_{daf}[a]	S_{daf}
57.89	6.44	3.46	32.21	82.45	4.94	1.01	10.48	1.11

[a]Calculated by the difference method.

samples are shown in Table 1. During the in situ pyrolysis of tar-rich coal, a wide-range distribution of particle size is present, possibly varying from the meter scale to the micron level. Here, from the lab-scale study, micron-sized particles were used to elucidate the pyrolysis and mild oxidation behaviors of tar-rich coal. Particles with sizes in the range of centimeters and decimeters should be further employed using larger-scale experimental devices, together with a meter magnitude in pilot-scale or industrial-scale studies in the future. The dry and ash-free volatile content of the experimental coal sample is 34.43%, which demonstrates that the tar-rich coal sample here is typical low-rank coal with an extremely low ash content. The high volatility and low ash content establish the advantage of extracting oil−gas resources. In addition, the carbon content is high but the hydrogen level is low. The high carbon-to-hydrogen ratio leads to a possible low level of light oil, and further upgrading is likely to be necessary after the devolatilization process.

A test of low-temperature carbonization of tar-rich coal was first carried out to obtain the tar yield, as shown in Table 2.

Table 2. Characteristics of the Char Residue and Low-Temperature Carbonization Analysis

	low-temperature carbonization/%		
characteristics of char residue, CRC	total water yield, $water_{ad}$	tar yield, tar_{ad}	semi-coke yield, $coke_{ad}$
2	15.0	9.1	66.5

The tar yield of the present example is 9.1%, which is approximately 30% of the sum of water vapor and volatile matter. The characteristics of the char residue represent the physical form of the residual solid after pyrolysis. The characteristic index of the char residue obtained in the present study is 2, which means that the residue can become powdery or almost powdery after being slightly touched by the finger. Hence, the semi-coke obtained from tar-rich coal does not have cohesiveness.

2.2. Analysis Methods. Thermogravimetric analysis is an extensively used method to evaluate thermal conversion behaviors of solid organic matter.[31−33] Here, the pyrolysis experiments were conducted using a synchronous thermogravimetric analyzer Labsys Evo. The mass of the solid sample in each test was 30 mg, and the total gas flow rate was 40 mL·min^{-1}. The experiments were carried out under several atmospheres: N_2, CO_2, 3% O_2/97% CO_2, 5% O_2/95% CO_2, 3% O_2/97% N_2, and 5% O_2/95% N_2. The sample temperature was increased from 30 °C to a preset temperature at heating rates of 0.5, 1, 5, 10, 15, and 20 °C·min^{-1}, respectively. The ultimate temperature varied from 450 to 700 °C every 50 °C, which corresponds to low-temperature pyrolysis of the tar-rich coal. The experiments adopted the single-factor controlled variable method. The parameters of standard conditions are an ultimate pyrolysis temperature of 600 °C, a heating rate of 5 °C·min^{-1}, and a N_2 atmosphere. Prior to the experiments, the benchmark experiments were carried out to eliminate the buoyancy effect and other factors resulting in a possible thermogravimetric curve drift.

After the pyrolysis experiments, the residual semi-coke samples were collected for subsequent analyses. A scanning electron microscope (SEM, JSM-7000F) was employed to analyze the micromorphology of particle surfaces. Fourier transform infrared spectroscopy (FTIR, Nicolet iS50) was applied to evaluate the organic functional groups of the residual semi-coke.

3. RESULTS AND DISCUSSION

3.1. Effects of Pyrolysis Temperature. The breaking of chemical bonds and formation of oil−gas components are highly dependent on the pyrolysis temperature. Figure 1 depicts the thermogravimetric analysis curves of tar-rich coal at various ultimate temperatures of pyrolysis at a heating rate of 5

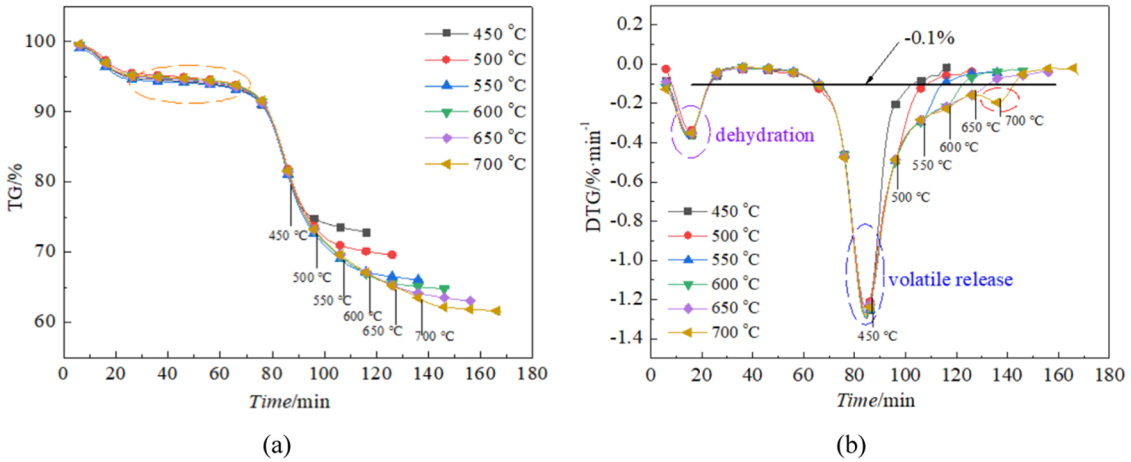

Figure 1. Effects of the ultimate temperature of pyrolysis on the thermal conversion of tar-rich coal at a heating rate of 5 °C·min^{-1} and under a N_2 atmosphere: (a) TG curves; (b) DTG curves.

https://doi.org/10.1021/acsomega.2c02786
ACS Omega 2022, 7, 25613−25624

°C·min^{-1} and under a N_2 atmosphere. It can be seen from Figure 1a that with the increase in the ultimate temperature of pyrolysis, the residue is reduced and mass loss is increased, with more volatile matter released. The increased extent of mass loss between 500 and 550 °C presents the maximum elevation, whereas the increased extent of mass loss from 550 to 700 °C is insignificant, as illustrated in Figure 2. The

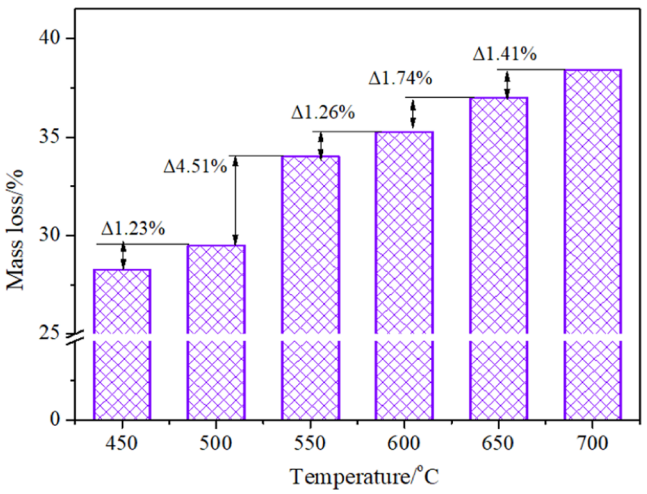

Figure 2. Variation of the final mass loss during the pyrolysis of tar-rich coal at various ultimate temperatures.

thermal decomposition of tar-rich coal is dominant between 500 and 550 °C, whereas the differences in organic hydrocarbon components in various coal types yield distinct effects in the temperature range of most severe pyrolysis reactions. Three stages can be observed on TG/DTG curves of tar-rich coal pyrolysis. At the first low-temperature stage, the release of moisture and adsorbed gas in the porous structure is predominant. At the second principal pyrolysis stage, the bridged linkages and aliphatic side chains within the hydrocarbon structure crack, together with the decomposition of the less thermally stable phenolic hydroxyl groups, and then plentiful gaseous hydrocarbons and tar vapor are discharged. As the pyrolysis temperature is further increased, polycondensation carbonization and secondary cracking proceed with more H_2 discharge.

The pyrolysis of tar-rich coal, in both underground in situ and aboveground carbonization circumstances, is a process of chemical-bound cracking and condensation. When the temperature is low, a weak bond cannot completely crack with the formation of a few volatiles, and consequently, the yield of coal tar is low. Higher temperatures lead to more release of volatile matters including both oil and gas components, whereas further increase in the ultimate temperature of pyrolysis possibly triggers secondary cracking of already-formed oil products to generate small-molecule gases and solids. The choice of the ultimate temperature of pyrolysis is not only associated with economic cost but also with the production quality. The product composition from tar-rich coal is largely temperature-dependent, and tar/oil components are favored at moderate temperatures, whereas high temperatures favor the gas yield.[18] Tar is formed mainly from the cleavage of macromolecular structures. If tar is the targeted product, the appropriate temperature of pyrolysis should be first tested for different coal types, including petrographic analysis, proximate analysis, organic components of coal, and so on. Wu et al.[28] found that the main pyrolysis process occurs in the temperature range of 300−600 °C. After reaching the starting temperature of tar-rich coal decomposition, the apparent specific heat could be significantly affected by the reaction mechanisms of coal pyrolysis.[29]

Figure 1b depicts a comparison of DTG curves at various ultimate temperatures of pyrolysis. The DTG curves are coincident at low temperatures, with the same dehydration and volatile peaks. An increase in the temperature promotes the release of volatiles. It is interesting that with further increase in the pyrolysis temperature to 700 °C, an additional peak appears on the DTG curve, which is possibly related to a change in the pyrolysis mechanism or/and decomposition of minerals. Partial minerals probably generate catalytic impacts on the cleavage of the macromolecular organic structure. Therefore, more detailed studies on inherent mechanisms and further elucidation are necessary.

Figure 3 shows the micromorphology of the residual semi-coke of tar-rich coal pyrolyzed at 450, 600, and 700 °C. From Figure 3a, a more developed porous structure can be observed on the semi-coke surface at 450 °C. The quick release of volatiles is beneficial for the formation of pores. Coal sometimes has a possible bedding architecture with nonlinear and anisotropic mechanical characteristics. Hence, the volatile matter is inclined to discharge from a certain direction, and the formation of pores in various directions holds different possibilities. As depicted in Figure 3a, one surface is abundant in porous structures whereas another has limited pores. The pores generated by pyrolysis are likely parallel to the direction of the coal bedding. The effect of direction is significant for the pyrolysis of large-scale underground coal bedding. As shown in Figure 3b,c, the porosity of the residual semi-coke exhibits limited variation as the temperature is increased from 600 to 700 °C. Consequently, most oil−gas components can be volatilized at 600 °C. From Figure 3c, it can be seen that the phenomenon of particle accumulation on the semi-coke surface is reduced by the presence of a smooth surface. It follows that a high temperature promotes the formation of a large hydrocarbon structure and then the generation of a carbon layer. According to the energy-dispersive spectrum (EDS) analysis, CaO was detected on the surface of the residual semi-coke obtained at 700 °C, as shown in Figure 3c. The decomposition of $CaCO_3$ is responsible for the formation of CaO. The decarbonation could give rise to more pores from the CO_2 release, but the alkaline earth metal products are likely to block pores due to their fouling nature in turn. The possible decomposition and interaction of minerals during the underground in situ pyrolysis of tar-rich coal should be considered, especially at high temperatures. The residual semi-coke left underground has a potential for CO_2 sequestration due to its well-developed porosity and large surface area, which benefits carbon neutrality.

The pyrolyzed semi-coke of tar-rich coal is a complicated mixture comprising multiple functional groups and various hydrocarbons together with residual minerals. The functional groups on the surface of the residual semi-coke vary with the heating process, and a deep understanding of the variation of these chemical structures benefits further interpretation of the organic matter transformation during the pyrolysis process. Figure 4 depicts the FTIR spectra of the residual semi-coke obtained at 450, 600, and 700 °C. The characteristic peaks and absorption bands in the infrared spectra are located mainly at 3550−3400, 1750−1500, and 1200−1000 cm^{-1}. The absorp-

https://doi.org/10.1021/acsomega.2c02786
ACS Omega 2022, 7, 25613−25624

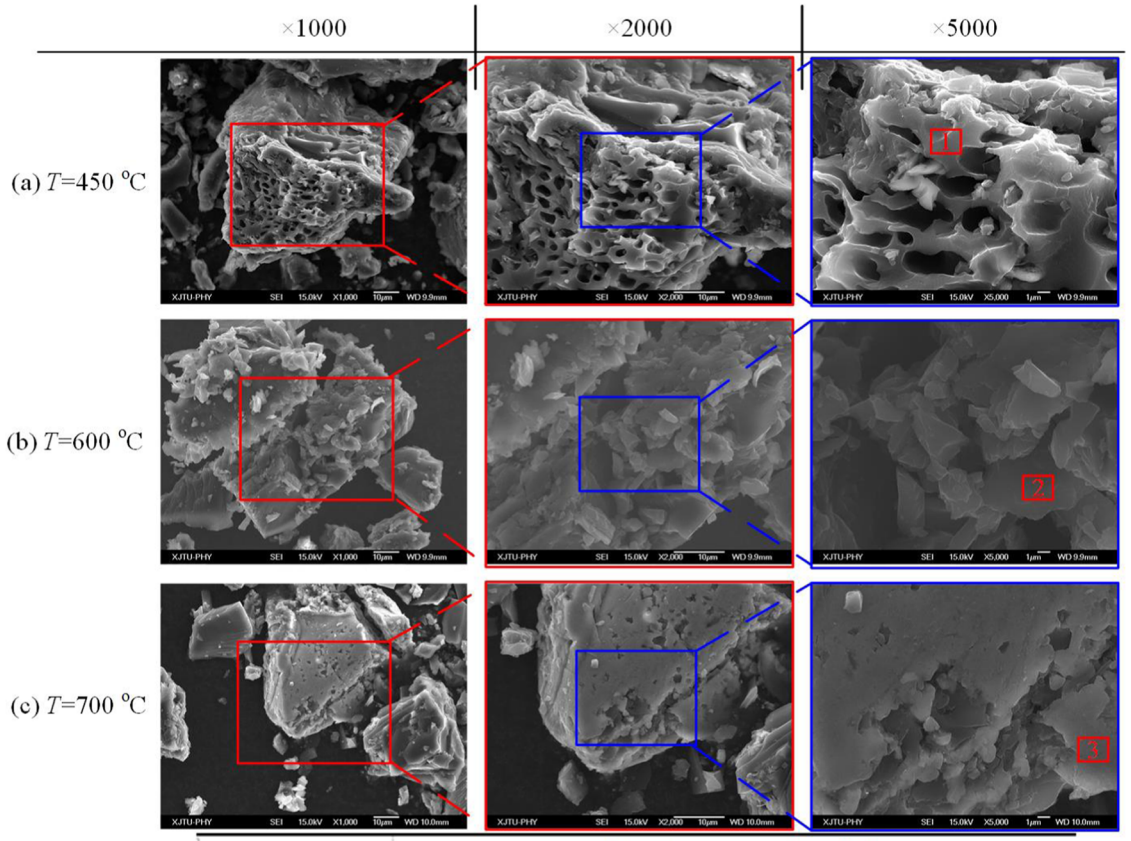

	Atomic percentage/%		
	C	Ca	O
Area 1	100	0	0
Area 2	100	0	0
Area 3	0	50.84	49.16

Figure 3. Micromorphology of the residual semi-coke from tar-rich coal at various temperatures: (a) T = 450 °C; (b) T = 600 °C; and (c) T = 700 °C.

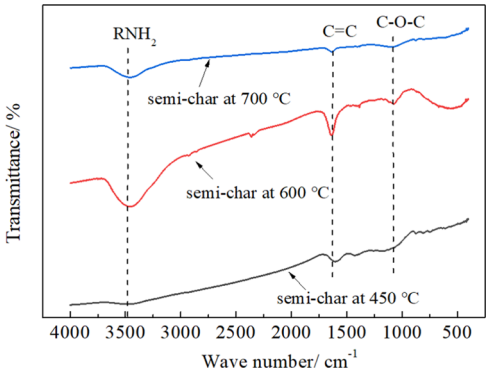

Figure 4. FTIR spectrum of the residual semi-coke from tar-rich coal at various temperatures.

tion peak of 3480 cm^{-1} is related to the amino group RNH_2, the absorption peak near 1605 cm^{-1} principally corresponds to stretching vibrations of carbon−carbon double bonds in benzene rings, and the absorption peak close to 1167 cm^{-1} is attributed to stretching vibrations of C−O−C bonds. The ultimate temperature of pyrolysis has a clear influence on the transformation of the organic matter in semi-coke, with a major impact on the peak intensity and not the absorption band type.

3.2. Influences of Pyrolysis Atmosphere. Several fluid mediums can be utilized to heat tar-rich coal underground, such as N_2, CO_2, flue gas, and water vapor. The specific heat capacity and thermal conductivity of various gases differ considerably from each other. The different atmospheres possibly have different dissolving capacities of in situ pyrolysis products, while they could also trigger different reactions within minerals and organic matters. Here, the pyrolysis under N_2 and CO_2 atmospheres was mainly emphasized. A small amount of oxygen permeation into the heating medium is inevitable under the complicated conditions of underground pyrolysis. In addition, the flue gas after the combustion process possibly could be utilized for underground pyrolysis of tar-rich coal. Hence, except for pure N_2 and CO_2 atmospheres, conditions with a small amount of O_2 were also compared to elucidate the contribution of limited O_2 to the pyrolysis behaviors of tar-rich coal.

Figure 5a depicts the TG/DTG curves of tar-rich coal pyrolysis in pure CO_2 at an ultimate temperature of 600 °C and a heating rate of 5 °C·min^{-1}. Similar to that under a N_2 atmosphere, only two obvious peaks of mass loss can be

https://doi.org/10.1021/acsomega.2c02786
ACS Omega 2022, 7, 25613−25624

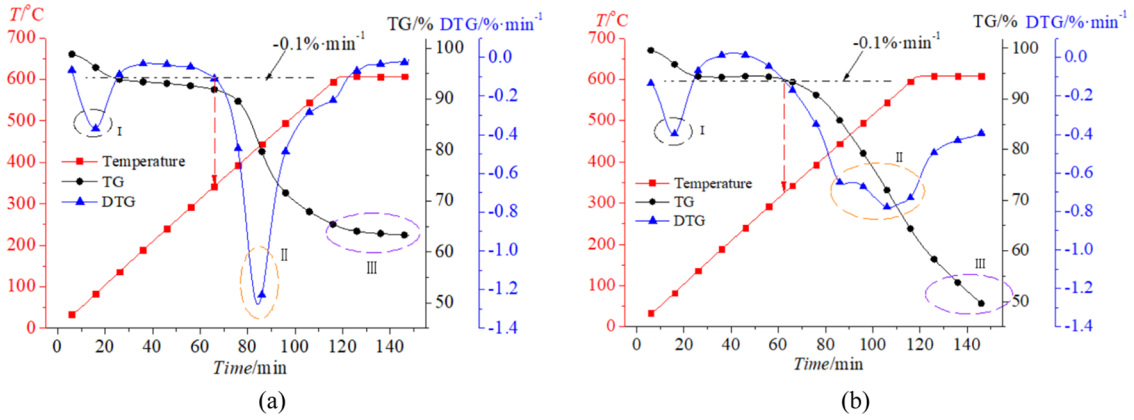

Figure 5. Comparison of TG/DTG curves of tar-rich coal pyrolysis under CO_2 and 3% O_2/97% CO_2 atmospheres at an ultimate temperature of 600 °C and a heating rate of 5 °C·min^{-1}: (a) CO_2 atmosphere; (b) 3% O_2/97% CO_2 atmosphere.

Table 3. Some Characteristic Parameters under Conditions of Various Atmospheres

atmosphere	CO_2	N_2	3% O_2/97% CO_2	3% O_2/97% N_2	5% O_2/95% CO_2	5% O_2/95% N_2
mass loss/%	36.74	35.27	52.17	53.82	62.95	69.24
DTG peak/(%·min^{-1})	−1.28	−1.29	−0.78	−0.85	−1.00	−1.12
T_{max}/°C	434	433	554	549	535	534

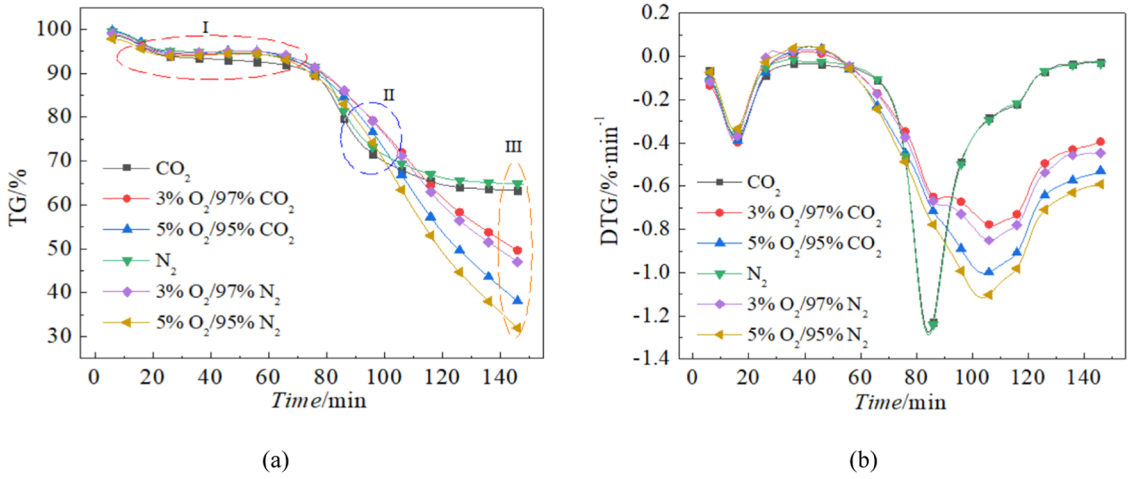

Figure 6. Influences of the atmosphere on TG/DTG curves of tar-rich coal pyrolysis at a heating rate of 5 °C·min^{-1} and an ultimate temperature of 600 °C: (a) TG curves; (b) DTG curves.

observed in the DTG curve. A temperature of 600 °C is insufficient for C−CO_2 gasification, and the pyrolysis behaviors in CO_2 highly resemble those in N_2, which is consistent with previous studies.[34] Carbon dioxide is a competitive heating medium during the in situ pyrolysis of tar-rich coal. Figure 5b demonstrates the mass loss curves of tar-rich coal under conditions of 3% O_2/97% CO_2. At the ultimate constant temperature of 600 °C, there is still a clear mass loss, which differs from the phenomenon in CO_2. This is attributed to the organic components undergoing not only pyrolysis but also slow oxidation. The oxidation reaction rate is positively correlated to the temperature and oxygen content. Therefore, the oxygen content in the carrier gas further noticeably promotes mass loss with an increase in the temperature. In addition, mass loss occurs under a 3% O_2/97% CO_2 atmosphere, but it is prolonged compared with that under a CO_2 atmosphere. The thermal conversion of tar-rich coal under a CO_2 atmosphere with limited O_2 includes both pyrolysis and slow oxidation, which can consume the light components and provide a certain amount of heat for the heating process. However, the addition of O_2 possibly further utilizes oil−gas products if the proper control cannot be obtained, which is also likely to reduce the yield of oil and gas from the in situ pyrolysis process. Hence, monitoring the temperature, atmosphere, and product distribution is important during the in situ pyrolytic exploitation of tar-rich coal.

The influences of the atmosphere on TG/DTG curves of tar-rich coal pyrolysis at an ultimate temperature of 600 °C and a heating rate of 5 °C·min^{-1} are illustrated in Figure 6. The mass loss with 3% O_2 is increased by 15−19% compared with that under an inert atmosphere, as displayed in Table 3. Three stages can be seen, as depicted in Figure 6a. In the presence of a small amount of oxygen, the oxidation process of the residual semi-coke proceeds, and the contribution of oxidation cannot be neglected. The heat released from oxidation can save the energy introduced from the external heating source, whereas it is likely to consume the volatile matter in turn. The mass loss under a N_2 atmosphere with a small amount of O_2 is greater

https://doi.org/10.1021/acsomega.2c02786
ACS Omega 2022, 7, 25613−25624

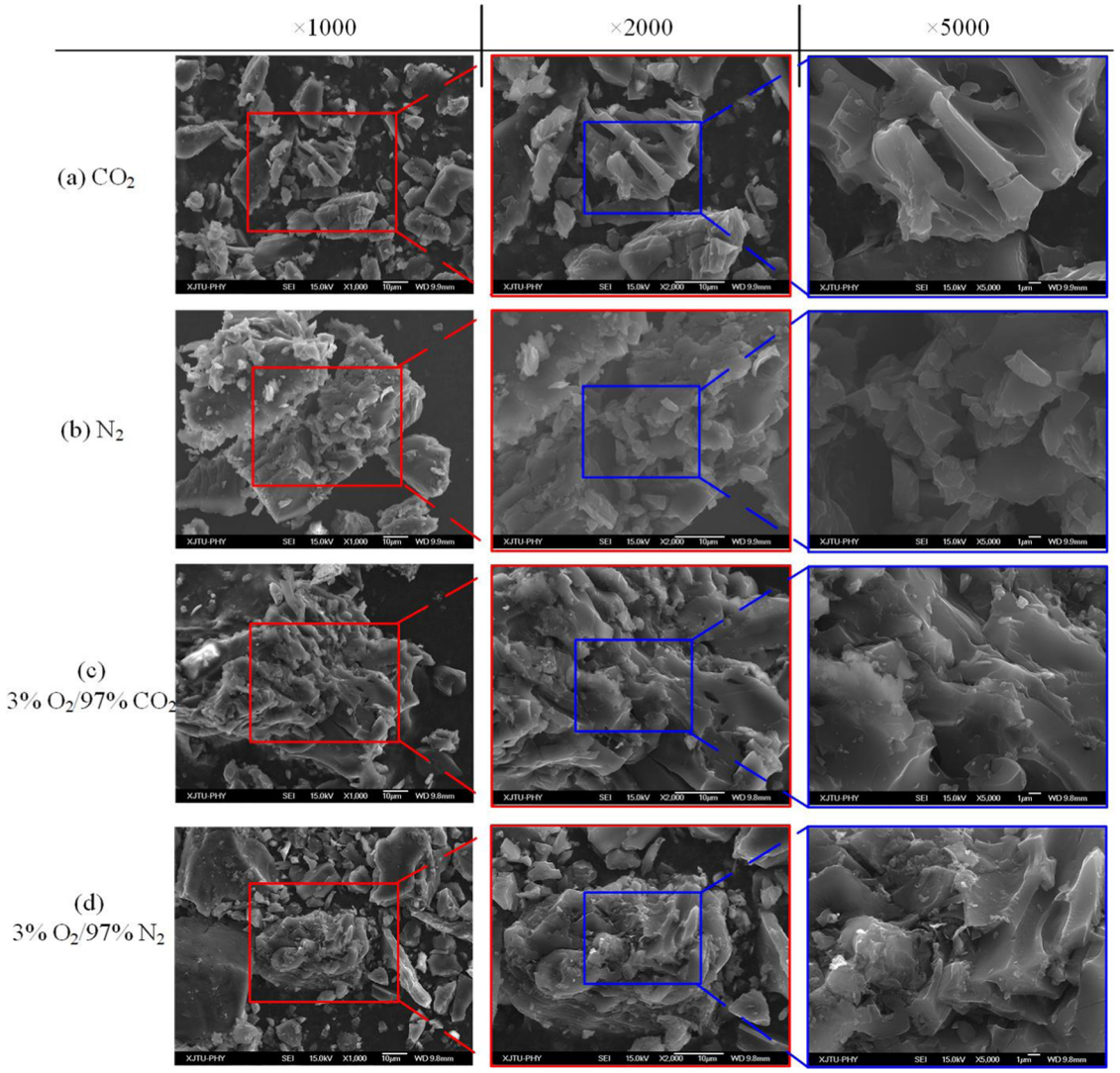

Figure 7. Micromorphology of the residual semi-coke of tar-rich coal pyrolyzed under various atmospheres at a heating rate of 5 °C·min^{-1} and an ultimate temperature of 600 °C: (a) CO_2; (b) N_2; (c) 3% O_2/97% CO_2; and (d) 3% O_2/97% N_2.

than that obtained under a CO_2 atmosphere, and the DTG peak values in the case of O_2/N_2 are greater than those obtained under an O_2/CO_2 atmosphere, as shown in Table 3. In the presence of CO_2, the oxidation reactions are weakened, which is due to the fact that the heat capacity of CO_2 is higher than that of N_2. The diffusivity of O_2 in CO_2 also differs from that in N_2. It can also be seen from Figure 6b that the mass loss peaks on DTG curves in the low-O_2 cases differ substantially from those without O_2. Compared with N_2 or CO_2 conditions, the maximum peaks are delayed in the presence of limited O_2, as against that under an inert atmosphere, whereas the duration of mass loss with oxygen is prolonged. In addition, because of the presence of O_2, the TG curves cannot reach constant values during the continuous slow oxidation.

Actually, the effects of additional CO_2 on the pyrolysis process are possibly susceptible to the temperature and CO_2 concentration.[23] Under a N_2 atmosphere, coal conversion can be accelerated because of char-CO_2 gasification at high temperatures,[35] whereas CO_2 has a negligible effect in promoting coal pyrolysis from the gasification process at low temperatures (<800 °C) by the underground in-situ pyrolysis. Nevertheless, Huanying et al.[23] observed that a high concentration of CO_2 inhibited coal pyrolysis at an ultrafast heating rate. A high level of CO_2 could be responsible for the cross-linking reaction, inhibition of the aromatic cluster, and then weakening of the pyrolysis reactions of coal samples.[36,37]

Figure 7 depicts the morphology of the residual semi-coke obtained from various atmospheres. Compared with Figure 7a,b, the particle surfaces in Figure 7c,d are rougher, with slightly enlarged particle sizes. A part of the organic material was oxidized or incinerated. A few macroscopic surfaces of semi-coke particles obtained from the atmosphere with a small amount of oxygen present a clear gray color, but only a dark color could be observed on the residual semi-coke from the inert atmosphere. With the oxidation of organic matter, the local temperature of the semi-coke particles is elevated, and then the possibility of mineral decomposition is promoted. The minerals formed can agglomerate on the particle surface, which induces the loss of the smooth surface and further adhesion. Not all organic matter can be excluded under the present experimental conditions.

As the temperature is below 800 °C, the C−CO_2 gasification reactions cannot take place apparently. Nevertheless, CO_2 could hinder the possible decomposition of minerals in tar-

https://doi.org/10.1021/acsomega.2c02786
ACS Omega 2022, 7, 25613−25624

Table 4. Some Characteristic Parameters under Conditions of Various Heating Rates Corresponding to Figure 8

heating rate	0.5 °C·min^{-1}	1 °C·min^{-1}	5 °C·min^{-1}	10 °C·min^{-1}	15 °C·min^{-1}	20 °C·min^{-1}
mass loss/%	32.39	31.93	35.27	35.99	35.78	35.75
DTG peak/%·min^{-1}	−0.09	−0.22	−1.29	−2.50	−3.83	−4.81
DTG peak/%·°C^{-1}	−0.19	−0.22	−0.26	−0.25	−0.26	−0.24
Total heating time/min	1170	600	144	87	68	58.5
T_{max}/°C	404	411	433	444	450	466

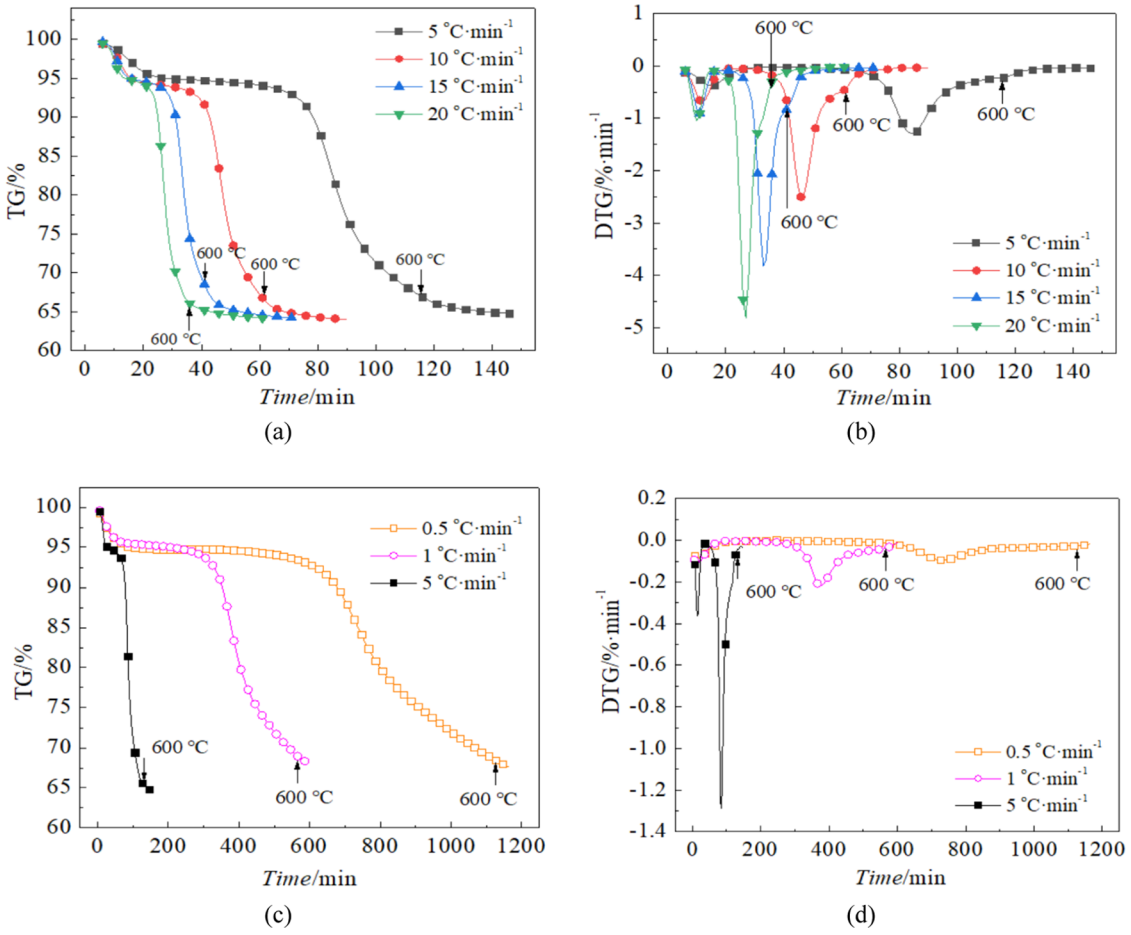

Figure 8. Influences of the heating rate on TG/DTG curves of tar-rich coal pyrolysis at an ultimate temperature of 600 °C under a N_2 atmosphere: (a) TG curves at heating rates of 5−20 °C·min^{-1}; (b) DTG curves at heating rates of 5−20 °C·min^{-1}; (c) TG curves at heating rates of 0.5−5 °C·min^{-1}; (d) DTG curves at heating rates of 0.5−5 °C·min^{-1}.

rich coal. Compared with the case of a N_2 atmosphere, the particle surfaces of semi-coke obtained under a CO_2 atmosphere are relatively smooth, while the differences in physical−chemical properties between N_2 and CO_2 are responsible for the observed phenomenon. CO_2 itself is the possible pyrolysis product, which also has an influence on the chemical reaction equilibrium. It can be deduced that the higher heat conductivity coefficient of CO_2 results in a faster heat transfer and then a decrease in the temperature difference between the internal and external surfaces, which possibly reduces the stress concentration and secondary reactions on particle surfaces. Except for the yield and morphology of semi-coke, the pyrolysis atmosphere also has a profound impact on volatile products, which requires further detailed evaluation. The liquid fuel yield can be significantly improved if a hydrogen-rich gas is employed to heat tar-rich coal, whereas more CO can be generated if CO_2 is used as the externally generated heating medium.[18]

3.3. Impacts of Heating Rate. The heating rate is one of the most important factors affecting the pyrolysis characteristics of solid fuels.[21,27,38] The practical pyrolysis process of tar-rich coal underground is varied and slow. The heating rate probably impacts the porous structure and then the characteristic parameters of pyrolyzed semi-coke. Here, the influences of the heating rate, especially slow rates of 0.5 and 1 °C·min^{-1}, on the pyrolysis process of tar-rich coal were investigated (Table 4).

Due to the extremely different durations under conditions of various heating rates, as shown in Table 4, with an ultimate temperature of 600 °C under a N_2 atmosphere, the TG/DTG curves of various heating rates are depicted in separate figures, with the heating rate of 5 °C·min^{-1} as the reference. As shown in Figure 8a and Table 4, the total mass loss at a heating rate of 5−20 °C·min^{-1} is almost unchanged. In Figure 8b, similar peaks of mass loss can be observed, whereas the mass loss rate per minute increases with an increase in the heating rate due to

https://doi.org/10.1021/acsomega.2c02786
ACS Omega 2022, 7, 25613−25624

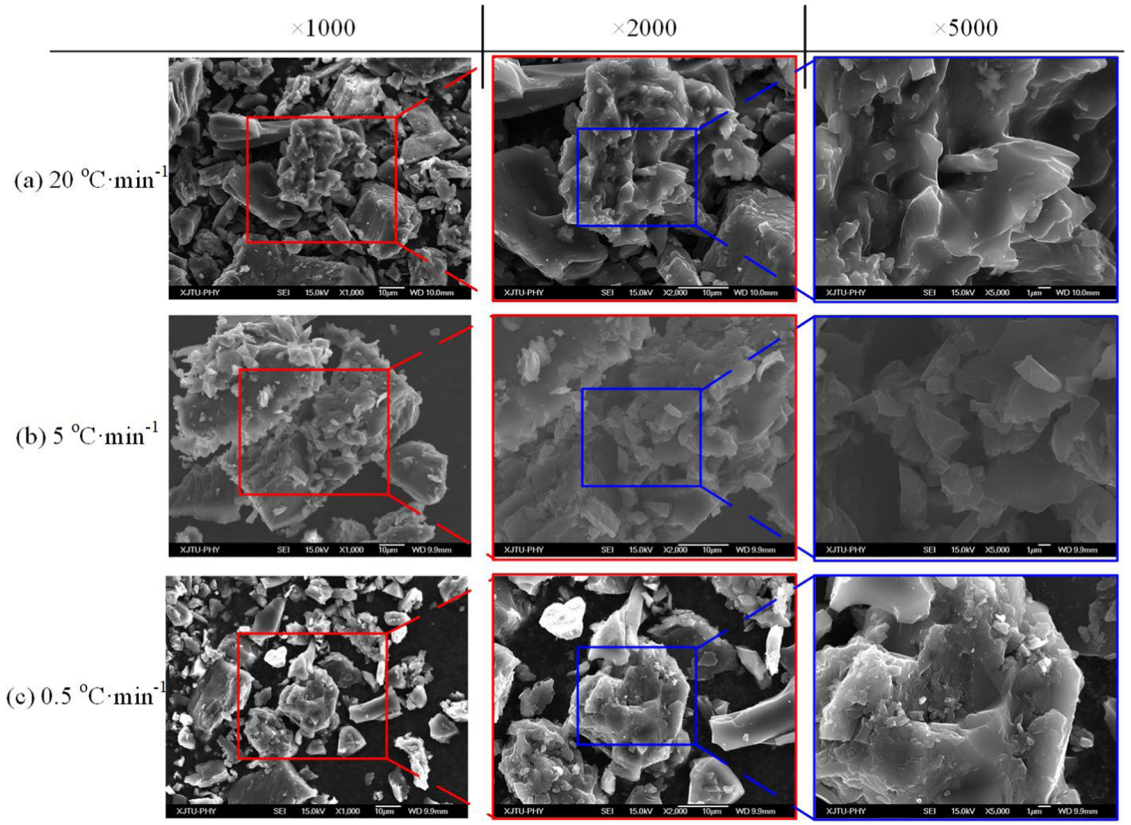

Figure 9. Micromorphology of the residual semi-coke of tar-rich coal pyrolyzed at various heating rates at an ultimate temperature of 600 °C under a N_2 atmosphere: (a) 20 °C·min^{-1}; (b) 5 °C·min^{-1}; and (c) 0.5 °C·min^{-1}.

the decrease in the heating duration. In addition, the temperature corresponding to the maximum mass loss peak (T_{max}) is positively associated with the heating rate, as shown in Table 4, which is because of thermal hysteresis.[39,40] Song et al.[21] found that the characteristic temperature of low-rank coal pyrolysis and the maximum mass loss rate increased with the heating rate increasing from 5 to 30 °C·min^{-1} under a N_2 atmosphere, which is in accordance with the present study. Huanying et al.[23] indicated that the mass loss rate at an ultrafast heating rate (1800 °C·min^{-1}) was elevated by several decuples compared with that at the traditional slow heating rate. The higher heating rate results in a shorter duration at certain temperatures, together with a more obvious hysteresis effect.[41] In addition, the heating rate possibly alters the peak distribution on the DTG curve of solid fuel pyrolysis. Nyoni et al.[42] compared the mass loss curves between heating rates of 10 and 50 °C·min^{-1} and found that the pyrolysis DTG curves were characterized by a single peak and multipeaks at high and low heating rates, respectively.

However, if the mass loss rate is converted into value per degree centigrade, the DTG peak values are quite similar under conditions of 5−20 °C·min^{-1}, as shown in Table 4. In addition, experiments at heating rates of 0.5 and 1 °C·min^{-1} were also performed to evaluate the pyrolysis behaviors at much lower heating rates. Although the pyrolysis duration time is prolonged at heating rates of 0.5 and 1 °C·min^{-1}, the mass loss at lower heating rates here is lower than those at rates above 5 °C·min^{-1}, as shown in Table 4. The decrease in the heating rate exerts a disadvantageous effect on the production of total volatiles. This is possibly because the temperature difference between the particle surface and the interior at a high heating rate leads to an increase in the porosity. However, the heat transfer is quite sufficient at a low heating rate, and the temperature distribution within the particles of tar-rich coal is uniform, with a limited formation of the porous structure. Okumura indicated that coal pyrolysis at a high heating rate could achieve a higher volatile yield than that with slow pyrolysis,[20] and Xu et al.[24] also concluded that an increase in the heating rate increased the mass loss and reduced the char yield, which are consistent with the results of the present study. However, Jayaraman et al.[26] believed that the pyrolysis heating rate had a significant influence on the curve of mass conversion and mass loss rate, but the total mass loss was almost unchanged with the heating rate. One interesting issue in the present investigation is that the mass loss presents a slight variation with a change in the heating rate from 5 to 20 °C·min^{-1}. Such a small difference of 15 °C·min^{-1} cannot effectively differentiate the impacts of the heating rate on the char yield and volatile production.

Table 4 shows some characteristic parameters under conditions of various heating rates corresponding to Figure 8. The mass loss rates per degree centigrade at heating rates of 0.5 and 1 °C·min^{-1} are clearly lower than those above a heating rate of 5 °C·min^{-1}. The extremely low heating rate brings about a possible change in the mechanism of chemical bond cracking during pyrolysis. In the industrial application of underground in-situ pyrolysis of tar-rich coal, the heating rate is possibly extremely low, which is not conducive to acquiring oil−gas products.

The micromorphology of residual semi-coke of tar-rich coal pyrolyzed at various heating rates is depicted in Figure 9 at an ultimate temperature of 600 °C and under a N_2 atmosphere.

https://doi.org/10.1021/acsomega.2c02786
ACS Omega 2022, 7, 25613−25624

More pores can be generated in tar-rich coal with an increased heating rate, which causes an increase in the roughness of the semi-coke surface and the growth of the porous structure. The heating rate has a considerable impact on the semi-coke reactivity. Generally, a higher heating rate leads to higher activity, which is mainly because the devolatilization process is more rapid at a higher heating rate. An increase in the devolatilization velocity increases the possibility of local fracture, thus enhancing the porous structure. Semi-coke is mainly comprised of a hydrocarbon skeleton and minerals. The morphology of semi-coke is principally determined by the skeleton near the particle surface, together with the formation and collapse of various pores. Here, the porous structure could be observed on surfaces of residual semi-coke at an ultimate temperature of 600 °C. Hence, it is easy to discharge volatiles from the organic components, and tar-rich coal is appropriate for oil−gas production.

The heating rate exerts an impact on the initiation of devolatilization. The beginning and maximum temperatures of volatiles are likely to increase with an increase in the heating rate. The pyrolysis of tar-rich coal is an endothermic reaction, and a thermal treatment time is necessary for the release of volatiles. With a high heating rate, the partial molecular structure of tar-rich coal cannot decompose in a timely manner, and the release of volatiles is delayed in the temperature-programmed process. Hence, the corresponding temperature of devolatilization is increased. The secondary reactions within the particle play an important role at a low heating rate, whereas the secondary reactions outside the particle contribute significantly to the overall process at a high heating rate. Hence, an increase in the heating rate leads to an enlarged pressure difference between the particle inside and outside, which gives rise to the fast release of volatiles and the development of a porous skeleton, as shown in Figure 9.

It can also be observed from Figure 9 that under conditions of greater magnification, through-holes are almost absent. As depicted in Figure 9c, abundant small particles attach to the carbon matrix, whereas the small particles adhering to the carbon skeleton diminish with an increase in the heating rate. From the EDS analysis, nearly only carbon elements were detected on the overwhelmingly major surfaces of the residual semi-coke, with a small amount of oxygen and hydrogen elements on residual surfaces. Consequently, 600 °C is adequate for particle surfaces of tar-rich coal to complete the pyrolysis process to produce tar. The residual semi-coke of tar-rich coal is mainly composed of a carbon skeleton, whereas a low mineral content is insufficient to form the characteristic skeleton structure of coal ash. The majority of mineral decomposition adheres to the matrix surface or embeds in the carbon skeleton. Gneshin et al.[6] studied the Utah bituminous coal undergoing pyrolysis under atmospheric pressure and indicated that the development of large pores associated with plastic swelling and deformation occurred at a heating rate of 10 °C·min^{-1} but did not occur at 0.1 °C·min^{-1}. Hence, the micromorphology of residual semi-coke after pyrolysis is susceptible to the heating rate. In addition, the heat and mass-transfer characteristics, the utilization of remnant heat within the residual char, the regulation of oil-gas products, and the capacity of CO_2 sequestration are still important issues for the development of underground thermal conversion technology of tar-rich coal.

4. CONCLUSIONS

In the present study, the pyrolysis and mild oxidation characteristics of tar-rich coal were investigated through thermogravimetric experiments, including the effects of low pyrolysis temperatures, varied pyrolysis atmospheres, and low heating rates, together with further physical−chemical analyses of the residual semi-coke. Experimental results indicate that the tar yield of the tar-rich coal is approximately 30% of the sum of the water vapor and volatile matter, whereas the residual semi-coke presents the absence of cohesion, which is largely influenced by the properties of the parent tar-rich coal. An increase in the ultimate temperature of pyrolysis leads to a decline in the residue mass with more volatile matter released. The increased extent of mass loss between 500 and 550 °C presents the maximum elevation. A high ultimate temperature benefits the release of volatile matters, whereas an excessive increase possibly triggers secondary cracking of already-formed oil products, which could reduce the yield of the targeted tar. The volatile matters are inclined to discharge from a certain direction, and the pores formed in various directions hold different possibilities, which are likely parallel to the coal bedding direction.

With a small amount of oxygen in the heating medium, the organic components undergo both pyrolysis and slow oxidation, which can consume the light components and provide a certain amount of heat. However, the addition of O_2 could further utilize oil-gas products and reduce the yield of oil−gas products if appropriate control cannot be achieved. Compared with an inert atmosphere, the mass loss under conditions of a small amount of O_2 is brought forward but prolonged. The mass loss under an O_2/N_2 atmosphere is greater than that obtained under an O_2/CO_2 atmosphere. The oxidation reactions of tar-rich coal are weakened in the presence of CO_2. With the oxidation of organic matter, the local temperature of semi-coke particles is elevated, and the formed minerals probably agglomerate on the particle surface.

The total mass loss under conditions of 5−20 °C·min^{-1} is almost unchanged, whereas the mass loss is clearly reduced as the heating rate is decreased to 1 °C·min^{-1}. The large reduction in the heating rate exerts a disadvantageous effect on the production of total volatiles. The extremely low heating rate brings about a possible change in the mechanism of chemical bond cracking during pyrolysis. More pores can be generated in tar-rich coal at an increased heating rate. The physical−chemical characteristics of residual semi-coke after pyrolysis are susceptible to the heating rate.

AUTHOR INFORMATION

Corresponding Author

Chang'an Wang − *State Key Laboratory of Multiphase Flow in Power Engineering, School of Energy and Power Engineering, Xi'an Jiaotong University, Xi'an 710049, China;* orcid.org/0000-0002-1730-740X; Email: changanwang@mail.xjtu.edu.cn

Authors

Li Ma − *Shaanxi Provincial Coal Geology Group Co. Ltd., Key Laboratory of Coal Resources Exploration and Comprehensive Utilization, Ministry of Natural and Resources, Xi'an 710026, China; School of Electrical Engineering, Xi'an Jiaotong University, Xi'an 710049, China*

https://doi.org/10.1021/acsomega.2c02786
ACS Omega 2022, 7, 25613−25624

Qisen Mao − *State Key Laboratory of Multiphase Flow in Power Engineering, School of Energy and Power Engineering, Xi'an Jiaotong University, Xi'an 710049, China*
Zhonghui Duan − *Shaanxi Provincial Coal Geology Group Co. Ltd., Key Laboratory of Coal Resources Exploration and Comprehensive Utilization, Ministry of Natural and Resources, Xi'an 710026, China*
Meijing Chen − *State Key Laboratory of Multiphase Flow in Power Engineering, School of Energy and Power Engineering, Xi'an Jiaotong University, Xi'an 710049, China*
Fu Yang − *Shaanxi Provincial Coal Geology Group Co. Ltd., Key Laboratory of Coal Resources Exploration and Comprehensive Utilization, Ministry of Natural and Resources, Xi'an 710026, China*
Jiamiao Liu − *State Key Laboratory of Multiphase Flow in Power Engineering, School of Energy and Power Engineering, Xi'an Jiaotong University, Xi'an 710049, China*
Zhendong Wang − *Shaanxi Provincial Coal Geology Group Co. Ltd., Key Laboratory of Coal Resources Exploration and Comprehensive Utilization, Ministry of Natural and Resources, Xi'an 710026, China*
Defu Che − *State Key Laboratory of Multiphase Flow in Power Engineering, School of Energy and Power Engineering, Xi'an Jiaotong University, Xi'an 710049, China;* orcid.org/0000-0003-1881-4136

Complete contact information is available at: https://pubs.acs.org/10.1021/acsomega.2c02786

Notes

The authors declare no competing financial interest.

■ ACKNOWLEDGMENTS

The financial support from the National Natural Science Foundation of China (No. 52176129) and the Research Project of Shaanxi Provincial Coal Geology Group Co., Ltd. (SMDZ-2020ZD-1−03) is sincerely acknowledged.

■ REFERENCES

(1) Qi, X. Y.; Li, Q. Z.; Zhang, H. J.; Xin, H. H. Thermodynamic characteristics of coal reaction under low oxygen concentration conditions. *J. Energy Inst.* **2017**, *90*, 544−555.
(2) Xin, H. H.; Wang, D. M.; Dou, G. L.; Qi, X. Y.; Xu, T.; Qi, G. S. The infrared characterization and mechanism of oxygen adsorption in coal. *Spectrosc. Lett.* **2014**, *47*, 664−675.
(3) Mathews, J. P.; Miller, B. G.; Song, C. S.; Schobert, H. H.; Botha, F.; Finkleman, R. B. The EBB and flow of US coal research 1970-2010 with a focus on academic institutions. *Fuel* **2013**, *105*, 1−12.
(4) Wang, C.; Zhao, L.; Yuan, M.; Wang, C.; Wang, P.; Du, Y.; Che, D. NO heterogeneous reduction on semi-coke and residual carbon with the presence of O_2 and CO. *Fuel* **2021**, *283*, No. 118954.
(5) Wang, S.; Shi, Q.; Wang, S.; Shen, Y.; Sun, Q.; Cai, Y. Resource property and exploitation concepts with green and low-carbon of tar-rich coal as coal-based oil and gas. *J. China Coal Soc.* **2021**, *46*, 1365−1377.
(6) Gneshin, K. W.; Krumm, R. L.; Eddings, E. G. Porosity and structure evolution during coal pyrolysis in large particles at very slow heating rates. *Energy Fuels* **2015**, *29*, 1574−1589.
(7) Shen, Y.; Wang, X.; Zhao, C.; Wang, S.; Guo, C.; Shi, Q.; Ma, W. Experimental study on multi-scale pore structure characteristics of tar-rich coal in Yushenfu mining area. *Coal Geol. Explor.* **2021**, *49*, 33−41.
(8) Ju, Y.; Zhu, Y.; Zhou, H. W.; Ge, S. R.; Xie, H. P. Microwave pyrolysis and its applications to the in situ recovery and conversion of oil from tar-rich coal: An overview on fundamentals, methods, and challenges. *Energy Rep.* **2021**, *7*, 523−536.
(9) Li, H.; Yao, Z.; Li, N.; Gao, J.; Xie, Q.; Wang, Q. Occurrence characteristics and resource potential evaluation of tar-rich coal for No.5∼(−2) coal seam in Shenfu mining area. *Coal Geol. Explor.* **2021**, *49*, 26−32.
(10) Zhang, N.; Xu, Y.; Qiao, J.; Ning, S. Organic geochemistry of the Jurassic tar-rich coal in Northern Shaanxi Province. *Coal Geol. Explor.* **2021**, *49*, 42−49.
(11) Ahmad, T.; Zhang, D. A critical review of comparative global historical energy consumption and future demand: The story told so far. *Energy Rep.* **2020**, *6*, 1973−1991.
(12) Xu, J.; Yang, Y.; Li, Y.-W. Recent development in converting coal to clean fuels in China. *Fuel* **2015**, *152*, 122−130.
(13) Lin, X. C.; Yin, J. A.; Luo, M.; Wang, C. H.; Wei, H.; Wang, Y. G. The catalytic hydrodesulfurization performance and mechanism of hierarchically porous iron-based catalyst for coal liquefaction oil. *Fuel Process. Technol.* **2022**, *228*, No. 107143.
(14) Kong, H.; Wang, J.; Zheng, H. F.; Wang, H. S.; Zhang, J.; Yu, Z. F.; Bo, Z. Techno-economic analysis of a solar thermochemical cycle-based direct coal liquefaction system for low-carbon oil production. *Energy* **2022**, *239*, No. 122167.
(15) Kalisz, S.; Kibort, K.; Mioduska, J.; Lieder, M.; Malachowska, A. Waste management in the mining industry of metals ores, coal, oil and natural gas-A review. *J. Environ. Manage.* **2022**, *304*, No. 114239.
(16) Ishaq, H.; Dincer, I. A new energy system based on biomass gasification for hydrogen and power production. *Energy Rep.* **2020**, *6*, 771−781.
(17) Restrepo, Á.; Bazzo, E.; Miyake, R. A life cycle assessment of the Brazilian coal used for electric power generation. *J. Cleaner Prod.* **2015**, *92*, 179−186.
(18) Zhang, H. R.; Li, S.; Kelly, K. E.; Eddings, E. G. Underground in situ coal thermal treatment for synthetic fuels production. *Prog. Energy Combust. Sci.* **2017**, *62*, 1−32.
(19) Kelly, K. E.; Wang, D.; Hradisky, M.; Silcox, G. D.; Smith, P. J.; Eddings, E. G.; Pershing, D. W. Underground coal thermal treatment as a potential low-carbon energy source. *Fuel Process. Technol.* **2016**, *144*, 8−19.
(20) Okumura, Y. Effect of heating rate and coal type on the yield of functional tar components. *Proc. Combust. Inst.* **2017**, *36*, 2075−2082.
(21) Song, H. J.; Liu, G. R.; Wu, J. H. Pyrolysis characteristics and kinetics of low rank coals by distributed activation energy model. *Energy Convers. Manage.* **2016**, *126*, 1037−1046.
(22) Wang, D.; Fletcher, T. H.; Mohanty, S.; Hu, H.; Eddings, E. G. Modified CPD model for coal devolatilization at underground coal thermal treatment conditions. *Energy Fuels* **2019**, *33*, 2981−2993.
(23) Huanying, C.; Hanjian, L.; Sheng, S.; Shagali, A. A.; Xiaoxue, A.; Jun, X.; Long, J.; Yi, W.; Song, H.; Jun, X. Effects of CO_2 and H_2O on coal pyrolysis with the ultrafast heating rate in a concentrating photothermal reactor. *J. Energy Inst.* **2021**, *98*, 44−52.
(24) Xu, S. P.; Zeng, X.; Han, Z. N.; Cheng, J. G.; Wu, R. C.; Chen, Z. H.; Masek, O.; Fang, X. F.; Xu, G. W. Quick pyrolysis of a massive coal sample via rapid infrared heating. *Appl. Energy* **2019**, *242*, 732−740.
(25) Duan, W. J.; Yu, Q. B.; Xie, H. Q.; Qin, Q. Pyrolysis of coal by solid heat carrier-experimental study and kinetic modeling. *Energy* **2017**, *135*, 317−326.
(26) Jayaraman, K.; Gokalp, I.; Bostyn, S. High ash coal pyrolysis at different heating rates to analyze its char structure, kinetics and evolved species. *J. Anal. Appl. Pyrolysis* **2015**, *113*, 426−433.
(27) Yan, B. H.; Cao, C. X.; Cheng, Y.; Jin, Y.; Cheng, Y. Experimental investigation on coal devolatilization at high temperatures with different heating rates. *Fuel* **2014**, *117*, 1215−1222.
(28) Wu, D.; Liu, G. J.; Sun, R. Y. Investigation on structural and thermodynamic characteristics of perhydrous bituminous coal by fourier transform infrared spectroscopy and thermogravimetry/mass spectrometry. *Energy Fuels* **2014**, *28*, 3024−3035.
(29) Strezov, V.; Lucas, J. A.; Evans, T. J.; Strezov, L. Effect of heating rate on the thermal properties and devolatilisation of coal. *J. Therm. Anal. Calorim.* **2004**, *78*, 385−397.

(30) Ju, Y.; Zhu, Y.; Xie, H.; Nie, X.; Zhang, Y.; Lu, C.; Gao, F. Fluidized mining and in-situ transformation of deep underground coal resources: a novel approach to ensuring safe, environmentally friendly, low-carbon, and clean utilisation. *Int. J. Coal Sci. Technol.* **2019**, *6*, 184−196.
(31) Kök, M. V.; Varfolomeev, M. A.; Nurgaliev, D. K. TGA and DSC investigation of different clay mineral effects on the combustion behavior and kinetics of crude oil from Kazan region, Russia. *J. Pet. Sci. Eng.* **2021**, *200*, No. 108364.
(32) Kok, M. V.; Varfolomeev, M. A.; Nurgaliev, D. K. Low-temperature oxidation reactions of crude oils using TGA-DSC techniques. *J. Therm. Anal. Calorim.* **2020**, *141*, 775−781.
(33) Jayaraman, K.; Kok, M. V.; Gokalp, I. Combustion mechanism and model free kinetics of different origin coal samples: Thermal analysis approach. *Energy* **2020**, *204*, No. 117905.
(34) Wang, C. A.; Zhang, X. M.; Liu, Y. H.; Che, D. F. Pyrolysis and combustion characteristics of coals in oxyfuel combustion. *Appl. Energy* **2012**, *97*, 264−273.
(35) Yi, B.; Zhang, L.; Huang, F.; Mao, Z.; Zheng, C. Effect of H_2O on the combustion characteristics of pulverized coal in O_2/CO_2 atmosphere. *Appl. Energy* **2014**, *132*, 349−357.
(36) Borrego, A. G.; Alvarez, D. Comparison of chars obtained under oxy-fuel and conventional pulverized coal combustion atmospheres. *Energy Fuels* **2007**, *21*, 3171−3179.
(37) Xu, J.; Su, S.; Sun, Z.; Si, N.; Qing, M.; Liu, L.; Hu, S.; Wang, Y.; Xiang, J. Effects of H_2O gasification reaction on the characteristics of chars under oxy-fuel combustion conditions with wet recycle. *Energy Fuels* **2016**, *30*, 9071−9079.
(38) Arenillas, A.; Rubiera, F.; Pevida, C.; Pis, J. J. A comparison of different methods for predicting coal devolatilisation kinetics. *J. Anal. Appl. Pyrolysis* **2001**, *58*−*59*, 685−701.
(39) Wang, C.; Du, Y.; Che, D. Reactivities of coals and synthetic model coal under oxy-fuel conditions. *Thermochim. Acta* **2013**, *553*, 8−15.
(40) Wang, C.; Zhao, L.; Yuan, M.; Du, Y.; Zhu, C.; Liu, Y.; Che, D. Effects of minerals containing sodium, calcium, and iron on oxy-fuel combustion reactivity and kinetics of Zhundong coal via synthetic coal. *J. Therm. Anal. Calorim.* **2020**, *139*, 261−271.
(41) Wang, G.; Zhang, J.; Shao, J.; Ren, S. Characterisation and model fitting kinetic analysis of coal/biomass co-combustion. *Thermochim. Acta* **2014**, *591*, 68−74.
(42) Nyoni, B.; Duma, S.; Shabangu, S. V.; Hlangothi, S. P. Comparison of the slow pyrolysis behavior and kinetics of coal, wood and algae at high heating rates. *Nat. Resour. Res.* **2020**, *29*, 3943−3955.

https://doi.org/10.1021/acsomega.2c02786
ACS Omega 2022, 7, 25613−25624